*Journal of Ceramic Processing Research. Vol. 17, No. 12, pp. 1226~1229 (2016)*

JOURNAL OF
**Ceramic Processing Research**

# Structure of hercynite prepared with existence of metal Fe

**Junhong Chen[a,*], Dongfang Liu[b], Mingwei Yan[a], Jindong Su[a], Bin Li[a] and Jialin Sun[a]**

[a]*School of Materials Science and Engineering, University of Science and Technology Beijing, Beijing 100083, China*

[b]*Department of Materials Science and Engineering, China University of Mining and Technology (Beijing), Beijing 100083, China*

**In this work, raw materials analytically pure $Al_2O_3$ and analytically pure $Fe_2O_3$ were mixed in FeO: $Al_2O_3$ molar ratio of 1 : 1 and pressed into specimens. The specimens were embedded in analytically pure metal Fe powders and fired slowly to 1650 °C in air atmosphere, and then soaked at 1650 °C for 5 hrs. The fired specimens were investigated by XRD, SEM, and EDS. The results show that the specimen synthesized at high temperatures in melting Fe is composed of hercynite and wüstite ($Fe_nO$ ($n \leq 1$)); $Fe_nO$ disperses in hercynite; hercynite crystals develop well and are mostly perfect octahedron with grain size around 50μm. The hercynite has Fe/Al ratio smaller than 1/2, which is non-stoichimetric. With the existence of melting Fe, although the raw materials are theoretically batched according to $FeO{\cdot}Al_2O_3$, $Fe_nO$ is still excess, so the hercynite obtained is Al-rich.**

**Key words: Melting Fe surrounding, Hercynite, Wüstite, Non-stoichiometric.**

## Introduction

Based on hercynite ($FeO{\cdot}Al_2O_3$) and periclase (MgO), periclase-hercynite is a chrome-free refractory for the burning zone of cement rotary kilns developed in recent years to meet the environmental-friendly requirement [1, 2]. It has excellent kiln coating ability as well as good structure flexibility and stress buffering ability, which is very suitable to be applied in the burning zone of rotary kilns [3-8]. So periclase-hercynite has become a main developing direction of refractories for the burning zone of rotary kilns. As the key starting material, hercynite is important but the synthesis of high grade hercynite is still difficult.

Up to now, various methods including reactive plasma sparying [9], pulsed laser ablation [10] and radial combustion of $Fe_2O_3$/aluminum thermite [11], reaction sintering [12], fused process [13] etc. have been adopted to synthesize hercynite, in which, reaction sintering and fused process are feasible to industrialize in refractories industry.

The key to synthesize hercynite is to control the stability of ferrous iron by sintering process and fused method. Element Fe in hercynite is divalent, but normally tervalent Fe is stable. FeO decomposes at temperatures below 570 °C [14]. Thus, at present, $Fe_3O_4$ or $Fe_2O_3$ is always used as the Fe source. During the synthesis, $Fe^{3+}$ is transformed into $Fe^{2+}$ by processing or controlling atmosphere then $Fe^{2+}$ reacts with $Al_2O_3$ to form hercynite.

However, the oxygen partial pressure range for FeO to exist is very narrow, as shown in Fig. 1 [15]. So the atmosphere control of reaction sintering is difficult, $Fe^{2+}$ is easy to transform into metal Fe or $Fe^{3+}$, resulting in impurities of metal Fe, magnetite, hematite, or residual corundum. The oxidation of metal Fe or magnetite as well as the volume expansion reaction between residual corundum and MgO deteriorates the properties of the products and leads to more rejected products [16]. In addition, the residual magnetite or hematite in the products results in multi-phase solid solution structure or multi-phase composited structure of the synthesized hercynite. So the effect of the hercynite on the properties of periclase-hercynite refractories as well as its own properties as a function of the temperature can be

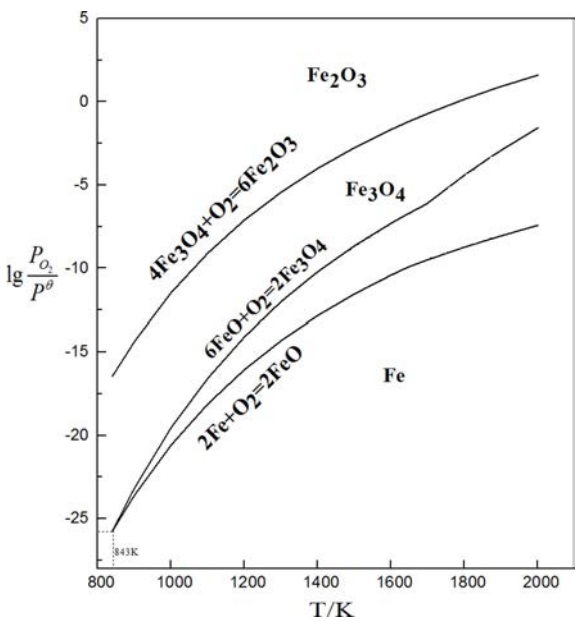


**Fig. 1** Thermodynamically stable area of Fe-O system.

*Corresponding author:
Tel : +86-13501163214
Fax: +86-010-62332666
E-mail: cjh2666@126.com

affected by many factors. The element diffusion, structure evolution, property change of the hercynite during atmosphere change as well as the structure change and reaction mechanism of hercynite in the periclase-hercynite refractories are difficult to describe. This is also the key restriction for the performance of hercynite in the periclase-hercynite refractories.

From Fig. 1, it is also found that at high temperatures and with the existence of metal Fe, the stable product between Fe and O is FeO, which means that in this condition with melting Fe, the oxide of Fe reacts with alumina to form high grade hercynite.

Hercynite is a kind of spinel which belongs to Fd3m crystal system. Its crystals have many vacancies which can hold many kinds of ions and form complicated solid solution [17, 18]. With the existence of melting Fe, the stoichiometry, microstructure and crystal morphology of the synthesized hercynite have not been reported. This is very important and fundamental for the preparation of high-purity, good crystallization and large size hercynite, the study of high purity hercynite on structure change during oxidation, the diffusion of hercynite in magnesia based materials, and using fused method to prepare high purity hercynite for mass production.

Therefore, in this work, hercynite was prepared at high temperatures with the existence of metal Fe. The structure, phase composition, atom ratios of the prepared hercynite were investigated to get some information on hercynite synthesized in equilibrium with metal Fe.

## Experimental

Analytically pure alumina ($\omega(Al_2O_3) > 99.3\%$) and analytically pure ferric oxide ($\omega(Fe_2O_3) > 99.5\%$) were adopted as raw materials, batched in FeO and $Al_2O_3$ molar ratio of 1 : 1. The batched materials were wet mixed in a planetary ball mill for 5h and then naturally air dried. The dried mixture was pressed into specimens with size of Φ20 mm × 20 mm under 10 MPa. The specimens were placed according to Fig. 2 and fired gradually to 1650 °C and soaked for 5 hrs.

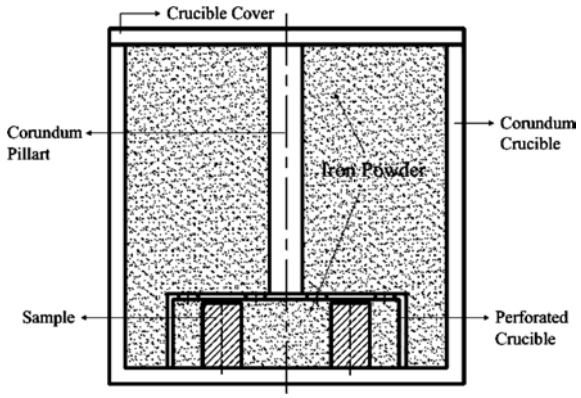


**Fig. 2.** Firing schematic diagram of specimens.

The fired specimens were sampled to analyze the phase composition and microstructure using an X-ray diffractometer (D8 ADVANCE, Bruker Corporation, scanning range of 15 °-100 °, scanning rate of 0.02 °/min) and a scanning electronic microscope (Quanta200, FEI, Holland) equipped with an energy dispersive spectrometer (INCA250 Oxford Instrument, UK).

## Results

### XRD analysis

The XRD pattern of the fired specimen is shown in Fig. 3. After firing at 1650 °C for 5hrs, the specimen is mainly composed of hercynite (Fe/Al < 1/2) and wüstite ($Fe_nO$). Since there are always more O atoms than Fe atoms in wüstite, the iron protoxide can be expressed as $Fe_nO$ (n < 1). This indicates that during the synthesis of hercynite, some ferric oxide does not participate in the crystal growth, leading to non-stoichiometric defected hercynite.

### SEM and EDS analysis

Fig. 4 shows the SEM images and EDS patterns of the specimen section. In Fig. 4(a), white substance and grey substance can be observed; the white substance disperses in the grey substance. The EDS analysis shows that the white substance is composed of Fe and O, and the grey substance consists of Fe, Al and O; Table 1 shows that Fe/Al < 1/2. So it is deduced that the white substance is wüstite and the grey substance is

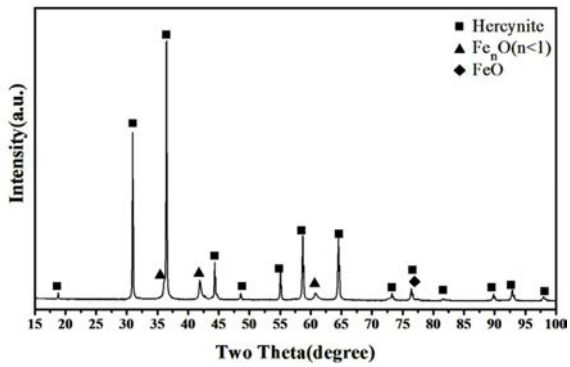


**Fig. 3.** XRD patterns of specimen fired at 1650 °C.

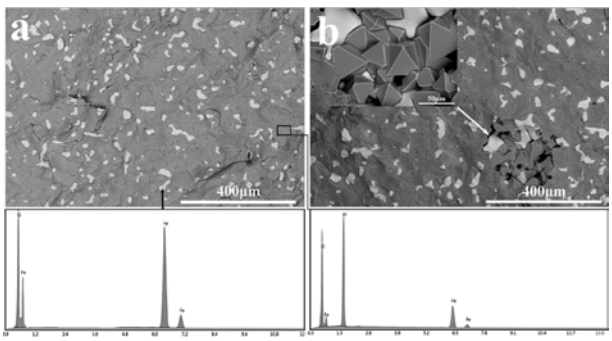


**Fig. 4.** SEM images and EDS patterns of specimen fired at 1650 °C

**Table 1.** EDS data of different microzones in specimen.

| EDS data number | The mole percent of different element /% | | | |
|---|---|---|---|---|
| | Fe | Al | O | |
| 1 | 14.52 | 29.69 | 55.79 | |
| 2 | 13.58 | 28.98 | 57.44 | |
| 3 | 13.90 | 28.18 | 57.92 | |
| 4 | 15.39 | 29.90 | 54.71 | |
| 5 | 12.34 | 28.41 | 59.25 | |
| 6 | 11.15 | 27.40 | 61.45 | |
| 7 | 13.72 | 29.56 | 56.72 | |
| 8 | 13.02 | 28.83 | 58.15 | |
| 9 | 13.31 | 29.02 | 57.67 | |
| 10 | 13.18 | 28.96 | 57.86 | |
| 11 | 11.59 | 27.99 | 60.42 | |
| 12 | 14.19 | 29.82 | 55.99 | Fe/Al < 1/2 |
| 13 | 14.36 | 29.80 | 55.84 | |
| 14 | 14.06 | 30.44 | 55.50 | |
| 15 | 13.17 | 29.08 | 57.75 | |
| 16 | 14.67 | 29.72 | 55.61 | |
| 17 | 11.95 | 28.26 | 59.79 | |
| 18 | 14.43 | 29.16 | 56.41 | |
| 19 | 14.11 | 29.78 | 56.11 | |
| 20 | 12.13 | 28.45 | 59.42 | |
| 21 | 12.49 | 28.60 | 58.91 | |
| 22 | 13.83 | 29.16 | 57.01 | |
| 23 | 12.96 | 29.27 | 57.77 | |
| 24 | 12.05 | 28.45 | 59.50 | |

defected hercynite. The hercynite is of perfect octahedron structure and the crystal size is about 50 μm.

## Analysis and Discussion

During the synthesis of hercynite, as temperature increases, the reaction between raw materials $Fe_2O_3$ and $Al_2O_3$ can be divided into two stages: (1) solid $Fe_nO$ reacts with $Al_2O_3$ forming hercynite; (2) liquid $Fe_nO$ reacts with $Al_2O_3$ forming hercynite.

### Solid $Fe_nO$ reacts with $Al_2O_3$ forming hercynite

Fe is valence-changeable; its oxides are different in different conditions (oxygen partial pressure and temperature). As shown in Fig. 5 [19], when the temperature is higher than 570 °C, iron protoxide exists in the form of wüstite ($Fe_nO$). To maintain an electric balance, some $Fe^{3+}$ exists. At 570-1371 °C which is the melting point range of $Fe_nO$, the composition of $Fe_nO$ ($n < 1$) in equilibrium with Fe changes according to curve QLJ as a function of temperature. So, at high temperatures with metal Fe embedded, when $Fe_nO$ exists in soilid state, wustite has more $O^{2-}$ and less $Fe^{2+}$.

Thus, as the system temperature increases, the wustite may react with $Al_2O_3$ to form hercynite as follows.

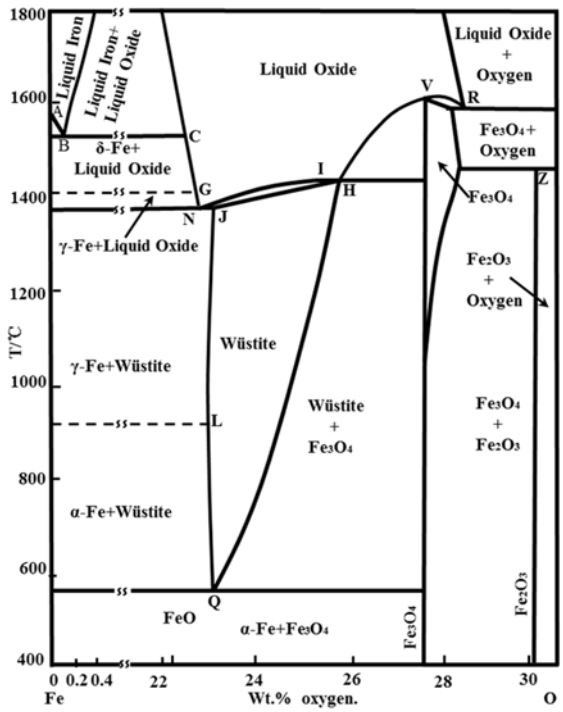


**Fig. 5.** Equilibrium phase diagram of Fe-O system.

$$Fe_nO(s)+Al_2O_3(s)=Fe_nO\cdot Al_2O_3(s) \quad (1)$$

$$\Delta G^{\theta}_{Fe_nO.Al_2O_3}=-30748-8.11T/J.mol^{-1}$$

(Note: the thermodynamic data of $Fe_nO$ adopt those of FeO)

As shown in the above thermodynamic calculation, this reaction can proceed before liquid appears in $Fe_nO$ (1371 °C). At the stage of solid-solid reaction, the formation of hercynite can be described by C. Wagher spinel formation modal [20]. The reaction between closely contacted solid FeO and $Al_2O_3$ particles can be considered as the mutual-diffusion between the hardly moved larger $O^{2-}$ ions and the smaller $Fe^{2+}$ and $Al^{3+}$ ions in the fixed oxygen packed structure [21].

On the $Al_2O_3$ side, $Fe^{2+}$ ($Fe^{3+}$) from wustite diffuses into crystal structure of $Al_2O_3$, resulting in the transformation of oxygen from hexagonal packing ($Al_2O_3$) to cubic packing (hercynite). On the $Fe_nO$ side, $Al^{3+}$ from $Al_2O_3$ diffuses into crystal lattice of $Fe_nO$, resulting in the adjusting of cation occupancy. Because the octahedral site preference energy sequence of $Al^{3+}$, $Fe^{2+}$ and $Fe^{3+}$ is $Al^{3+} > Fe^{2+} > Fe^{3+}$, during the formation of spinel, $Al^{3+}$ occupies octahedron sites of oxygen packing in priority. $Fe^{2+}$ in wustite can only occupy tetrahedron sites. Since $Fe^{2+}$ has larger radius than $Fe^{3+}$, the entrance of $Fe^{2+}$ in tetrahedron sites slightly changes the surrounding octahedron structure and further changes the surrounded tetrahedron. Small $Fe^{3+}$ is easy to enter the slightly changed tetrahedron, forming symmetric structure, thus hercynite with stable structure forms.

The existence of $Fe^{3+}$ in wustite makes the Fe/O ratio offset the theoretical value 1, so during the formation of hercynite, compared with the stoichiometric FeO, wustite provides less $Fe^{2+(3+)}$ ions for its reaction with $Al_2O_3$ which forms hercynite. This means that less $Fe^{2+(3+)}$ ions can diffuse to the $O^{2-}$ packing skeleton, the hercynite lattice with $Fe^{2+(3+)}/Al^{3+} < 1/2$ forms, i.e. the defected hercynite structure.

**Liquid $Fe_nO$ reacts with $Al_2O_3$ forming hercynite**

For liquid $Fe_nO$, as the temperature increases, its composition changes along the NGC curve as shown in Fig. 5. Although compared with that in QLJ, the $Fe_nO$ liquid composition in NGC has obviously reduced $O^{2-}$ content, the $O^{2-}/Fe^{2+(3+)}$ ratio is still larger than 1, i.e. there are more $O^{2-}$ ions and less $Fe^{2+(3+)}$ ions in the structure. Thus, similar with the hercynite formed by solid $Fe_nO$, the hercynite formed by liquid $Fe_nO$ is Al ion rich and Fe ion lack.

Based on the above analysis, no matter the solid-solid reaction or the liquid-solid reaction, because of the existence of $Fe^{3+}$, for $Fe_nO$, $n < 1$. So the hercynite synthesized at high temperatures with metal Fe embedded is Al rich defected spinel ($Fe_nAl_2O_4$) and some $Fe_nO$ remains in the material. Results of XRD (Fig. 3), SEM and EDS (Fig. 4) all prove this and confirm the existence of defected spinel, which is consistent with the study of Woodland, et al. [22].

Wustite in the hercynite synthesized in this work has two kinds of structure, namely the non-stoichiometric $Fe_nO$ (N, $n < 1$) and stoichiometric FeO (S). This is consistent with the study of A. Pattek-Janczyk, et al. [23]. The contents of the two kinds of wustite depend on the cooling rate. Generally, for rapid cooling, only N structure exists and S rarely, as the cooling slows down, S increases and N decreases gradually.

In this work, although the raw materials are batched according to $FeO?Al_2O_3 = 1 : 1$ in molar ratio, some wustite remains in the prepared hercynite. The residual wustite results in a large volume change in the periclase-hercynite brick because of the valence change ($Fe^{2+} \Leftrightarrow Fe^{3+}$), thus generating cracks in bricks and deteriorating performance of the bricks. The cracking of the periclase-hercynite brick is an unsolved problem and the main reason is the formation of $Fe_nO \cdot Al_2O_3$ ($n < 1$).

## Conclusions

Hercynite was synthesized by using analytically pure $Al_2O_3$ and analytically pure $Fe_2O_3$ as raw materials in $FeO : Al_2O_3$ molar ratio of 1 : 1, and firing at 1650 ºC for 5 hrs in a high temperature furnace. The results show that at high temperatures and with the existence of melting Fe, although the raw material is stoichimetrically batched, the hercynite specimen synthesized consists of hercynite ($Fe/Al < 1/2$) and $Fe_nO$ ($n \leq 1$) and $Fe_nO$ disperses in the hercynite; the hercynite crystals develop well, mostly in perfect octahedron with grain size around 50 μm. The Fe/Al ratio of the hercynite is smaller than 1/2, which proves the hercynite obtained is non-stoichimetric and Al-rich.

## Acknowledgments

The authors express their appreciation to National Nature Science Foundation of China (No. 51172021) and the National Science-technology Support Plan Projects (Grant 2013BAF09B01).

## References

1. J. Chen, M. Yan, J. Su, B. Li, Y. Li, Z. Li, J. Sun, D. Liu, J. Chin. Ceram. Soc. 43[3] (2015)340-344.
2. G. Liu, N. Li, W. Yan, G. Tao, Y. Li, J. Ceram. Process. Res. 13[4] (2012)480-485.
3. H. Liu, N. Li, Q. Li, China's Refractories 14[2] (2005)23-26.
4. K. Imai, H. Kusunose, I. Kenmochi, N. Kanni, K. Sakaguchi, Taikabutsu overseas (1998) 94-95.
5. J.E. Contreras, G.A. Castillo, E.A. Rodríguez, T.K. Das, A.M. Guzmán, Mater. Charact. 54[4-5] (2004) 354-359.
6. P. M. Botta, E.F. Aglietti, J.M.P. López, Mater. Chem. Phys. 76[1] (2002) 104-109.
7. Y.B. Pithawalla, M.S.E. Shall, S.C. Deevi, Intermetallics 8[9-11] (2000)1225-1231.
8. G. Buchebner, T. Molinaria, H. Harmuth, Proceedings of the Unified Int. Tech. Conf. On Refractories (UNITECR´99). (1999) 201-203.
9. Y. Yang, D.R. Yan, Y.C. Dong. X.G. Chen, L. Wang, Z.H. Chu, J.X. Zhang, J.N. He, J. Alloys Compd. 579 (2013) 1-6.
10. G.A.C. Rodriguez, G.G. Guilluen, M.I.M. Palma, T.K.D. Roy, A.M.G. Hernandez, J. Appl. Ceram. Technol. 12 (2015) E34-E43.
11. L. Durães, B.F.O. Costa, R. Santos, A. Correia, J. Campos, A. Portugal, Mater. Sci. Eng. A 465[1] (2007) 199-210.
12. J. Chen, L. Yu, J. Sun, Y. Li, W. Xue, J. Eur. Ceram. Soc. 31[3] (2011)259-263.
13. A. Paesano, C.K. Matsuda, J.B.M.D. Cunha, M.A.Z. Vasconcellos, B.Hallouche, S.L.S ilva, J. Magn. Magn. Mater. 264 [2-3] (2003) 264-274.
14. Z.Chen, J. Chai, Y. Li, Refractories 39(2005)207-210.
15. L.S. Darken, R.W. Gurry, J. Am. Chem. Soc. 68 (2002) 798-861.
16. J.H. Chen, M.W. Yan, J.D. Su, B. Li, Y. Li, J.L. Sun, J. Chin. Ceram. Soc. 43[9] (2015) 1284-1288.
17. I. Jastrzębska, J. Szczerba, P. Stoch, A. Błachowski, K. Ruebenbauer, R. Prorok, E.Śnieżek, Nukleonika. 60[1] (2015) 47-49.
18. J.R. Smyth, D.L. Bish, in "Crystal Structures and Cation Sites of the Rock-Forming Minerals" (Allen and Unwin, Boston, 1988).
19. Y. Fei, S.K. Saxena, Phys. Chem. Miner. 13[5] (1986) 311-324.
20. C. Wagner, J. Chem. Soc., Faraday Trans. 34 (1938) 851-859.
21. Z. He, Y. Yang, Acta Mineralogica Sinica. 17[3] (1997) 321-328.
22. K. Schollenbruch, A.B.Woodland, D.J.Frost, Phys. Chem. Miner. 37[3] (2010) 137-143.
23. A. Pattek-Janczyk, J.C. Grenier, B. Miczko, Solid State Ionics. 117[117] (1999) 95-103.